ELSEVIER

Journal of Photochemistry and Photobiology A: Chemistry 137 (2000) 9–14

Journal of Photochemistry and Photobiology A:Chemistry

www.elsevier.nl/locate/jphotochem

Photoinduced intramolecular charge transfer of 3-cyano-4-furyl-6-phenyl-2-(9-anthralylidene)-pyridine

Maged A. EI-Kemary

Department of Chemistry, Faculty of Education, Tanta University, Kafr El-Sheikh 33516, Egypt

Received 25 May 2000; received in revised form 23 June 2000; accepted 17 July 2000

Abstract

The absorption and fluorescence spectra, fluorescence quantum yields and lifetimes of 3-cyano-4-furyl-6-phenyl-2-(9-anthralylidene)-pyridine (FPAP) in various solvents are reported. The results show that the quantum yield of the fluorescence (Φ_f) of FPAP is high and decreased with increasing solvent polarity. The fluorescence decay time is almost single exponential, independent of the excitation wavelength and its value decreases upon increasing the solvent polarity. The radiative rate constant (k_r), however, shows a maximum value for solvents of intermediate polarity, e.g. in $CHCl_3$ a value of $2.1 \times 10^8\ s^{-1}$ is attained. However, k_{nr} value increases with increasing solvent polarity. The bathochromic shift of the emission spectra and the resulting increase in the excited state dipole moment indicate the charge transfer (CT) character of the emitting singlet state of FPAP. The relatively large values of k_r and the corresponding transition dipole moment (M_f) indicate the absence of a twist intramolecular charge transfer in the fluorescent states.

Keywords: Schiff base; Fluorescence lifetime; Dipole moment; Photoinduced charge transfer

1. Introduction

Photoinduced intramolecular charge transfer has been attracting considerable attention as a topic of central importance in photochemistry [1–8]. The excited state electron transfer in organic donor–acceptor molecules is usually described in terms of electronic coupling between the locally excited (LE) state, reached by Frank–Condon excitation of the ground state, and the charge transfer (CT) state. This process will lead to a large increase of the dipole moment, and hence will result in a marked solvatochromic effect and a large Stokes shift. 3-Cyano-4-furyl-6-phenyl-2-(9-anthralylidene)-pyridine (FPAP) is a fluorescent Schiff base showing intramolecular charge transfer upon excitation. Aromatic Schiff bases have attracted much attention due to their interesting photochemical [9,10] properties, in addition, to their use in the photographic field [11,12] and have also been found to exhibit pharmacological activities such as anti-inflammatory against carrageenan edema [13]. Recently, we have studied the electron transfer and charge transfer processes in various donor–acceptor systems upon excitation [14–16].

In this paper, we report the photophysical properties of new fluorescence probe, 3-cyano-4-furyl-6-phenyl-2-(9-anthralylidene)-pyridine (FPAP), whose fluorescence maximum shifts to larger wavelengths and fluorescence quantum yield decreases with increasing solvent polarity. This compound also have long emission wavelengths, high quantum yields and large Stokes shifts. Such fluorescent compound is obviously promising probe for certain applications: laser dayes, probes for micellar and biological systems, molecules for non-linear optics and photographic imaging.

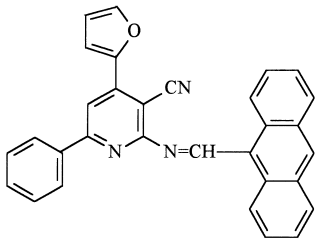

FPAP

2. Experimental

FPAP was synthesized by high temperature condensation of 2-amino-3-cyano-6-phenyl-4-(2′-furyl)-pyridine with 9-anthraldhyde. The former compound was prepared according to Ref. [17]. The purity of FPAP has been confirmed by spectroscopic and chromatographic technique.

All solvents used were analytical or spectroscopic grade of highest available purity and supplied by Merck, BDH or

1010-6030/00/$ – see front matter
PII: S1010-6030(00)00336-1

Aldrich. Ethyl acetate was washed with a standard Na_2CO_3 solution and distilled from CaH_2.

The fluorescence quantum yields were obtained using 9,10-diphenylanthracene in cyclohexane ($\Phi_f = 0.94$, $\lambda_{ex} =$ 380 nm) as standard [18]. The values of Φ_f for FPAP were obtained using the following relation

$$\Phi_f^u = \Phi_f^s \left(\frac{I^u}{I^s}\right)\left(\frac{n^u}{n^s}\right)^2$$

in which I is the fluorescence intensity and n is the refractive index of the solvent. The subscripts "s" and "u" refer to standard and unknown, respectively.

Unless otherwise stated, the experiments were performed at 25°C. The FPAP concentrations were in the range $(0.5–1.0) \times 10^{-5}$ M that no concentration quenching could be observed in the lifetimes.

The absorption and fluorescence spectra were recorded, respectively, on a Shimadzu 240 UV–VIS spectrophotometer and a Shimadzu RF-540 spectrofluorometer. The fluorescence lifetimes were measured with time-correlated single photon counting fluorimeter (Edinburgh Instruments, Model OB900). The half width of the instrument response was 1.0 ns. A synchronization photomultiplier was used for detection of fluorescence. The decay curves were analyzed by a multiexponential iterative fitting program. The goodness of the fit was estimated from an examination of χ^2, weighted residuals and auto-correlation functions.

3. Results and discussion

3.1. Absorption and emission spectra

The absorption and fluorescence spectra of FPAP were studied in different solvents and the experimental results are compiled in Table 1. The absorption spectra of FPAP in cyclohexane and *N*,*N*-dimethylformamide (DMF), presented in Fig. 1, consists of three absorption bands. The long wavelength absorption band at 380 nm loss structure, broadens and exhibits a slight red shift of 7 nm, upon increasing the solvent polarity from cyclohexane to DMF. However, the red shift in the longest wavelength band of FPAP as compared to that of the isolated anthracene unit [19], suggests that there is already an interaction between the anthralylidene and the substituted pyridine components in the ground state.

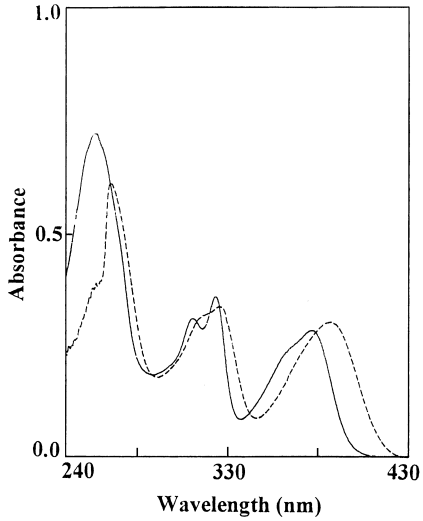

Fig. 1. Absorption spectra of FPAP in cyclohexane (—) and DMF (---).

Fig. 2 shows the fluorescence emission spectra of FPAP in some selected solvents of various polarity at room temperature. As can be seen in Table 1 and Figs. 1 and 2, the polarity of the solvent has a larger effect on the emission band maxima (λ_{max}^F) of FPAP than on the absorption band maxima (λ_{max}^A) This observation indicates that photoinduced intramolecular charge transfer (ICT) takes place within the molecule in the singlet excited state in comparison with the ground state. The presence of a single emission band indicates a barrierless electron transfer process and the slight shift and broadening of the absorption band in solvents

Table 1
Spectral properties and fluorescence quantum yield (Φ_f) of FPAP in different solvents

Solvent	λ_{max}^A nm, ($\epsilon_{max} \times 10^{-4}$ M^{-1} cm^{-1})	λ_{max}^F nm	$\Delta\nu \times 10^{-3}$ cm^{-1}	Φ_f[b]	Δf
DMF	268, 318(s), 328, 387 (1.71)[a]	430	2.58	0.53	0.275
Acetonitrile	258, 315(s), 323, 380 (1.63)[a]	424	2.73	0.55	0.305
Methanol	257, 315(s), 325, 383 (1.32)[a]	424	2.52	0.56	0.309
Ethanol	258, 315(s), 325, 384 (1.34)[a]	421	2.29	0.58	0.302
2-Propanol	258, 314(s), 326, 384 (1.20)[a]	420	2.23	0.60	0.276
n-Butanol	258, 313(s), 326, 384 (1.24)[a]	424	2.46	0.68	0.263
CH_2Cl_2	258, 315(s), 326, 378 (1.59)[a]	412	2.18	0.67	0.218
$CHCl_3$	259, 315(s), 326, 380 (1.47)[a]	411	1.98	0.67	0.148
Ethyl acetate	257, 313(s), 324, 382 (1.32)[a]	414	2.02	0.69	0.200
1,4-Dioxane	259, 314(s), 325, 384 (1.39)[a]	420	2.23	0.68	0.028
Decalin	257, 313(s), 326, 379 (1.42)[a]	405	1.69	0.75	0.002
Toluene	282, 316(s), 327, 383 (1.35)[a]	418	2.18	0.70	0.013
Cyclohexane	257, 313(s), 324, 380 (1.51)[a]	406	1.68	0.73	0.000

[a] Estimated at longer wavelength band, (s) is shoulder.
[b] $\lambda_{ex} = 380$ nm.

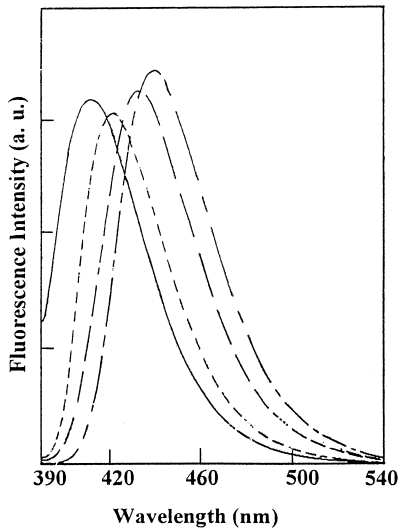

Fig. 2. Fluorescence emission spectra of FPAP as a function of solvent polarity at room temperature (λ_{ex} = 380 nm): cyclohexane (—), $CHCl_3$ (---), ethanol (— —) and DMF (— –).

of increasing polarity shows that the Franck–Condon LE state relaxes to a state with some CT character. The increase of the Stokes shift with increasing the solvent polarity also points to the CT character of the fluorescence states and clearly indicates that the excited state dipole moment of the FPAP is much higher than that of the ground state.

According to Lippret [20,21] and Mataga [22], the Stokes shift ($\Delta\nu = \nu_A - \nu_F$) (in cm^{-1}) should be linearly correlated with the solvent polarity function Δf defined as

$$\Delta f = \frac{\varepsilon - 1}{2\varepsilon + 1} - \frac{n^2 - 1}{2n^2 + 1} \quad (1)$$

where ε is the dielectric constant and n is the refractive index of the solvent. Their values were taken from Lange's handbook [23]. The slope of the straight line is given by [22]

$$s = \frac{2(\mu_e - \mu_g)^2}{hca^3} \quad (2)$$

where a is the radius (in Å) of the spherical cavity in Onsager's theory of reaction field, h is Planck's constant, and c is the speed of light. From the absorption and fluorescence spectra recorded in different solvents, it is possible to calculate the difference between the dipole moment in the excited and the ground state, $\Delta\mu = \mu_e - \mu_g$. Linear least-squares analysis of $\Delta\nu$ versus Δf (Fig. 2) yields

$$10^{-3}(\nu_A - \nu_F) = 2.78\Delta f + 1.63 \qquad (r = 0.91) \quad (3)$$

with $a \cong 9.5$ Å, the difference $\Delta\mu$ is found to be 15 D. Solvents such as 1,4-dioxane and toluene show deviation from linearity, probably due to specific solute–solvent interactions, are excluded from the evaluation. The high $\Delta\mu$ value of FPAP reveals a strong increase in the excited state dipole moment and confirming the CT character of the excited state.

The other most effective and practical polarity scale is Reichardt–Dimroth's $E_T(30)$ scale [24], which takes both polarity of the solvent and specific (hydrogen-bonding) interactions into account. A least-squares analysis for plotting of $\Delta\nu$ against $E_T(30)$, leads to the following relationship

$$\Delta\nu \times 10^{-3} = 0.03E_T(30) + 1.0$$
$$\text{(correlation coefficient } r = 0.71)$$

The relatively poor correlation between $\Delta\nu$ and $E_T(30)$ ($r = 0.71$) in comparison with Δf could indicate that the energy gap between the ground state and Franck–Condon excited state responsible for the electronic transition is mostly dependent on the polarity of the solvent and the hydrogen-bonding ability exerts little effect.

3.2. Fluorescence quantum yield and lifetime

As shown in Table 1, the fluorescence quantum yields of FPAP strongly depend upon the solvent polarity. In low polarity solvents (Δf = 0–0.2) or chlorinated ones (Δf = 0.148–0.218), the quantum yield (λ_{ex} = 380 nm) lies between 0.74–0.67. It decreases steadily with increasing polarity of the solvents. A plot of the quantum yield (Φ_f) versus solvent polarity (Δf) of FPAP shows an even better linear correlation (Fig. 4A) than the Stokes shift plot (Fig. 3). An equally satisfactory linear correlation was also found when the scale based on the empirical solvent parameter $E_T(30)$ of Dimroth [24] was used. The fluorescence quantum yield decreases steadily as the $E_T(30)$ increases, Fig. 4B.

Using single curve analysis, the fluorescence decay of FPAP could be analyzed as a single exponential decay in all solvents (except in toluene, where double decay is observed), as shown by values of χ^2 approaching 1.0 and random distribution of weighted residuals. The fluorescence lifetime is independent of the excitation as well as monitored emission wavelength in the solvents studied. An example is shown in Fig. 5, which presents a representative plot of the logarithm

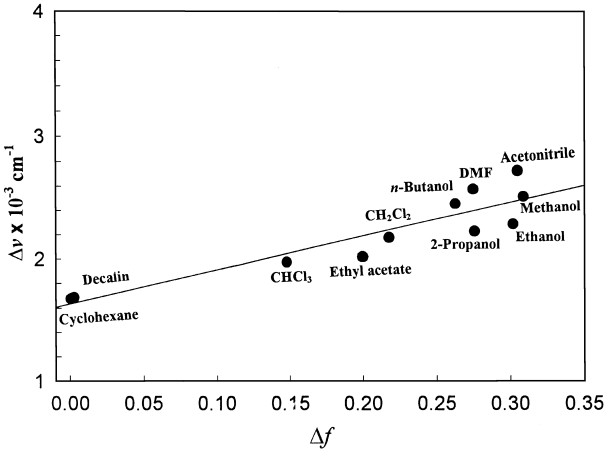

Fig. 3. Stokes shift of FPAP as a function of the polarity parameter Δf.

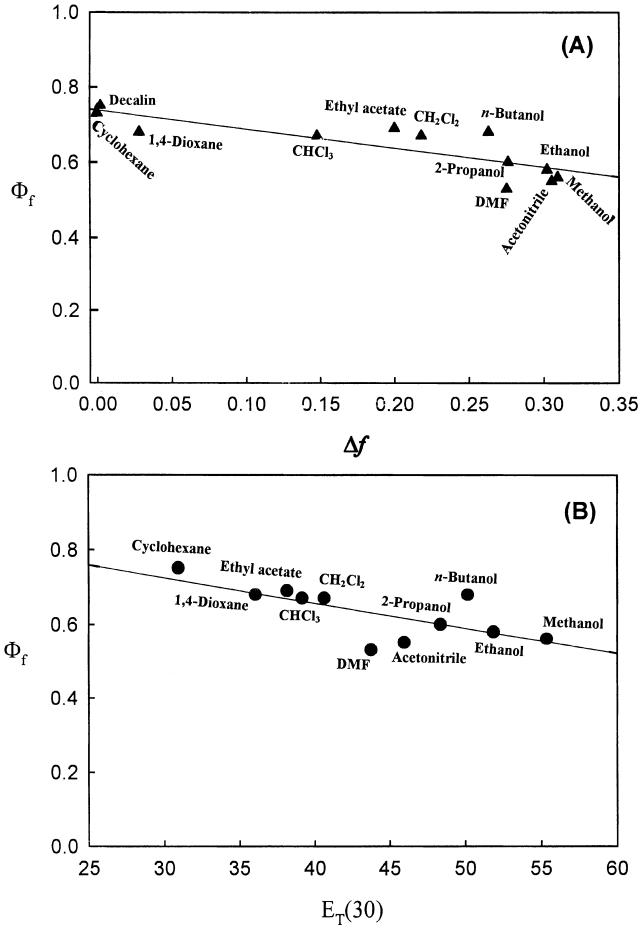

Fig. 4. Plot of Φ_f ($\lambda_{ex} = 380$ nm) for FPAP versus: (A) Δf; (B) $E_T(30)$.

of the relative fluorescence intensity versus time of FPAP in ethanol and toluene, from which the lifetimes of the excited singlet states, τ_f were obtained by iterative reconvolution of the measured instrument response function.

Table 2
Decay parameters of FPAP in various solvents

Solvent	τ_f (ns)[a]	χ^{2b}	$k_r \times 10^{-8}\ s^{-1}$	$k_{nr} \times 10^{-8}\ s^{-1}$	$\lvert M_f \rvert$ (D)[c]
DMF	3.35	1.02	1.6	1.4	2.8
Acetonitrile	3.59	1.16	1.5	1.3	3.0
Methanol	3.33	1.14	1.7	1.3	3.5
Ethanol	3.49	1.02	1.7	1.2	3.2
2-Propanol	3.30	1.19	1.8	1.2	3.3
n-Butanol	3.55	1.18	1.8	1.0	3.2
CH_2Cl_2	3.30	1.13	2.0	1.0	3.1
$CHCl_3$	3.23	1.20	2.1	1.0	3.1
Ethylacetate	3.77	1.21	1.8	1.0	3.2
1,4-Dioxane	3.75	1.13	1.8	0.9	3.0
Decalin	4.33	0.98	1.7	0.6	2.2
Toluene	4.37, 0.18	1.19	1.6	0.7	2.2
Cyclohexane	4.31	1.19	1.7	0.6	2.2

[a] λ_{ex}=380 nm.
[b] χ^2 is the reduced chi-square.
[c] 1 D (debye) $\approx 3.33564 \times 10^{-30}$ C m.

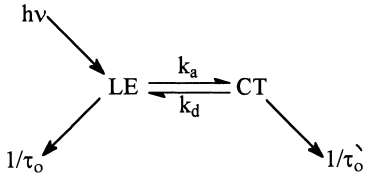

Scheme 1.

In Table 2, the decay times τ_f of FPAP is reported as a function of the solvent polarity. As can be seen, τ_f is significantly affected by the nature of the solvents; in non-polar solvents such as cyclohexane and decalin, it amounted to 4.31 and 4.33 ns, respectively. In polar solvents as acetonitrile and DMF the decay times amounted to 3.59 and 3.35 ns, respectively.

Fig. 6A shows an analysis of the distribution of fluorescence decay times of FPAP in ethanol where a narrow distribution is obtained. Similar results were obtained for FPAP in other solvents (except for toluene) examined in this work. The single exponential decay of FPAP and the corresponding narrow distribution can be explained by the presence of single excited state. This indicates that the LE→CT reaction barrier is low.

However, the double decay of FPAP in toluene (Fig. 5B) and the corresponding double distributions (Fig. 6B) indicates that the ICT interaction of FPAP and toluene is described by equilibrium between LE and CT states [25] according to Scheme 1.

Where k_a and k_d are the forward and backward reaction rate constants. $1/\tau_o$ and $1/\tau_o$, are the reciprocal lifetimes of the LE and CT states respectively. The decay times τ_1 and τ_2 and their amplitudes A_1 and A_2 are determined by the double exponential function using the following equation

$$I(t) = A_1 \exp\left(\frac{-t}{\tau_1}\right) + A_2 \exp\left(\frac{-t}{\tau_2}\right) \quad (4)$$

The longer value $\tau_1 = 4.37$ ns ($A_1 = 97.15\%$), is very close to those of single exponential analysis of FPAP in non-polar solvents. Hence the shorter lifetime $\tau_2 = 0.18$ ns ($A_2 = 2.85\%$), can be assigned to the LE state. The rate constants of the forward (k_a) and backward (k_d) ICT reactions can be determined in an approximate manner from $k_a/k_d = A_2/A_1$ [26]; where the ratio $A_2/A_1 = 0.029$. The evaluated reaction rates are as follows: $k_a = 1.57 \times 10^8\ s^{-1}$ and $k_d = 5.40 \times 10^9\ s^{-1}$. The larger back reaction rate k_d indicates a reversible reaction.

The high quantum yields of fluorescence and the relatively short decay times correlate with the highly allowed nature of the emissive CT state [26] and contrast with the rather forbidden emission associated with a twist intramolecular charge transfer TICT state [27,28].

The rate constants of radiative (k_r) and non-radiative (k_{nr}) deactivations were calculated from the quantum yield (Φ_f) and lifetime values according to classical relations

$$k_r = \frac{\Phi_f}{\tau_f} \quad (5)$$

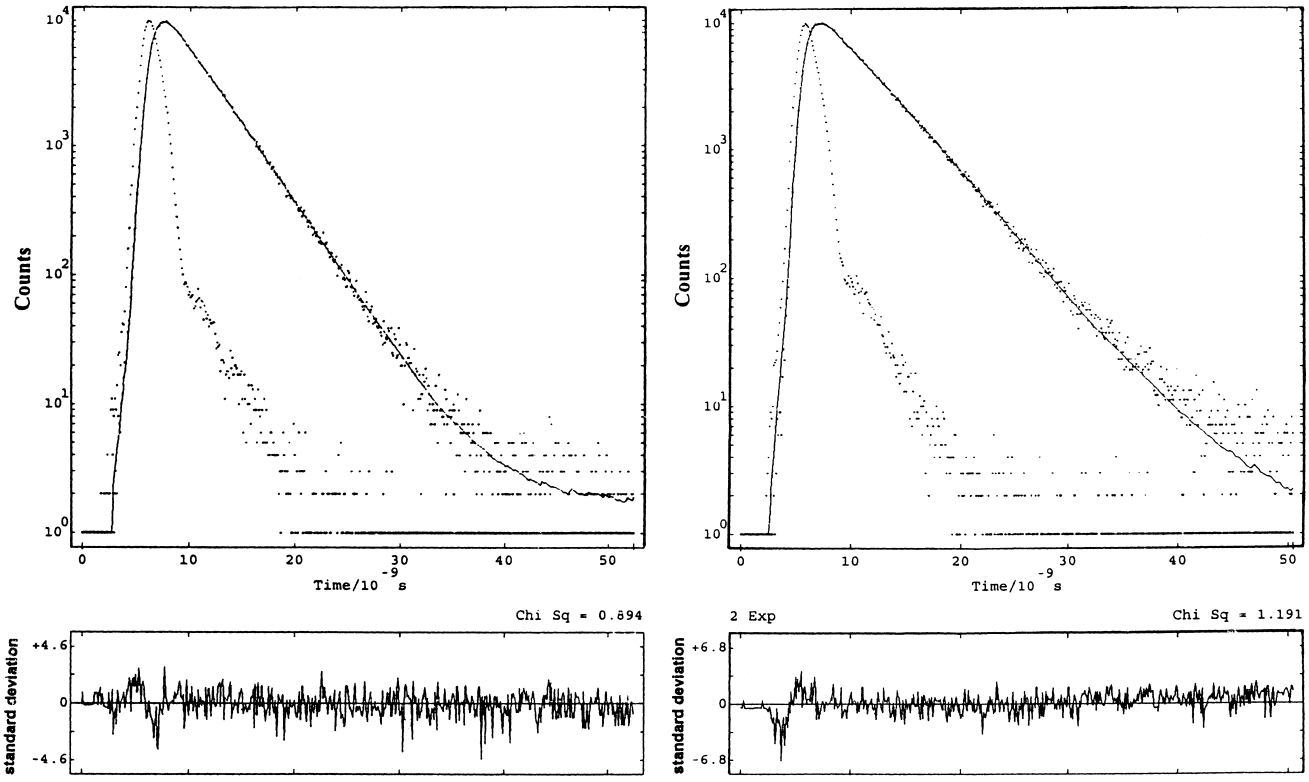

Fig. 5. Fluorescence decays and weighted residuals and auto-correlation functions for single exponential analysis of FPAP in ethanol (left) and double exponential analysis in toluene (right) solutions at room temperature.

and

$$k_{nr} = \frac{(1 - \Phi_f)}{\tau_f} \quad (6)$$

The k_r and k_{nr} values are summarized in Table 2. The evaluated k_r values show a maximum for solvents of intermediate polarity such as CH_2Cl_2 and $CHCl_3$. In contrast, regular increase of k_{nr} is observed with increasing polarity of the solvent.

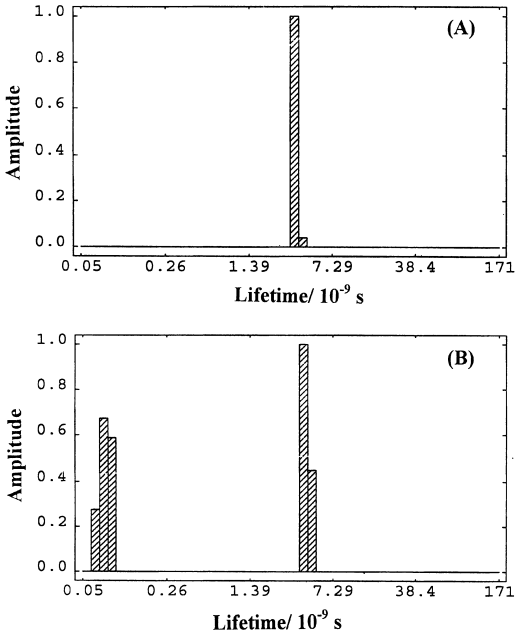

Fig. 6. Lifetime distributions of FPAP at room temperature: (A) in ethanol; (B) in toluene.

The $S_1 \rightarrow S_0$ transition dipole moments M_f, which are related to the radiative rate constant k_r can be calculated using the equation [20,21]

$$k_r = \frac{64\pi^4}{3h} n^3 \nu_f^3 |M_f|^2 \quad (7)$$

where, h is the Planck constant, n is the refractive index of the solvent and ν_f is the wavenumber of the emission. The values of M_f are given in Table 2. It should be noted, however, that the transition dipole moment M_f, extracted from the data measured in polar solvents are significantly larger than those resulting from the data obtained from non-polar solvents, indicating that the electronic dipole moment value is dependent on the emitted energy (see Table 2). Typical dependence of M_f on the CT fluorescence energy ν_f is presented in Fig. 7.

This finding also shows that the relaxed emitting state in polar solvent contain a strongly allowed character due to the contribution of the locally excited configurations and thus implies a moderate change in geometry of the CT state with respect to the LE state. This results in ruling out the TICT mechanism in FPAP.

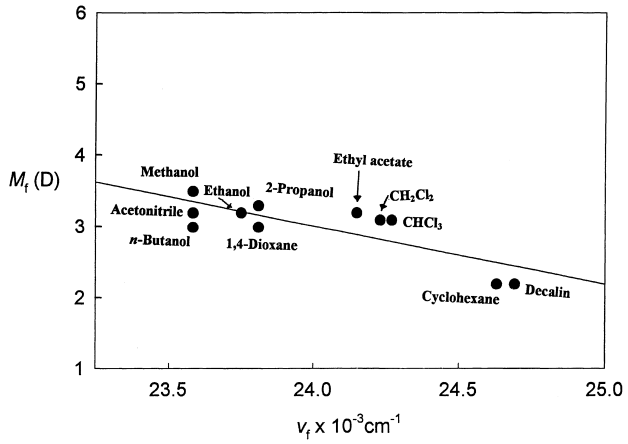

Fig. 7. Correlation between the transition dipole moment M_f of FPAP and the fluorescence CT energy ν_f in various solvents.

3.3. Temperature dependence of the CT fluorescence band maximum and the spectral bandwidth

The effect of temperature of the CT emission spectra of FPAP was investigated in chloroform. The shape of the CT band and its width at half maximum as well as its position do not change when the temperature is raised from 288 to 308 K. This behavior agree well with the previous findings that FPAP does not undergo any significant low-frequency intramolecular nuclear motion upon excitation. Thus, the twist angle between the donor and acceptor moieties in the emitting CT state seems to be similar with that in the ground state. This hypothesis is strongly supported by the large value of the fluorescence rate constants (k_r) and the corresponding transition dipole moments (M_f).

4. Conclusions

The bathochromic shift of the emission spectra of FPAP and the resulting increase in the excited state dipole moment are clear evidence that the excited state has a pronounced charge transfer character. The large Stokes shifts, large values of radiative rate constants and the corresponding transition dipole moments as well as the temperature independence of the fluorescence profiles and bandwidth of the fluorescence spectrum ruled out the TICT mechanism of the emitting state.

The presence of a single emission band indicates a barrierless electron transfer process. The slight shift and the broadening of the absorption in solvents of increasing polarity shows that the Franck–Condon LE state relaxes to a state with some CT character.

References

[1] A. Kapturkiewicz, J. Herbich, J. Karpiuk, J. Nowacki, J. Phys. Chem. A 101 (1997) 2332.
[2] D. Braun, W. Rettig, S. Delmond, J.F. Letard, R. Lapouyade, J. Phys. Chem. A 101 (1997) 6836.
[3] K. Zachariasse, M. Grobys, E. Tauer, Chem. Phys. Lett. 274 (1997) 372.
[4] Ý.V. Il'ichev, W. Kuhnle, K.A. Zachariasse, Chem. Phys. Lett. 211 (1996) 441.
[5] M. Maroncelli, J. Mcinnis, G.R. Fleming, Science 243 (1989) 1679.
[6] F. Lahmani, E. Bréhéret, A. Zehnacker-Rentien, J.F. Delouis, O. Benoist d'Azy, J. Photochem. Photobiol. A: Chem. 89 (1995) 191.
[7] A. Onkelinex, F.C. De Schryver, L. Viaene, M. Van der Auweraer, K. Iwai, M. Yamamoto, M. Ichikawa, H. Masuhara, M. Maus, W. Rettig, J. Am. Chem. Soc. 119 (1996) 2892.
[8] P.F. Barbara, G.C. Walker, T.P. Smith, Science 256 (1992) 975.
[9] G. Pistolis, D. Gegiou, E. Hadjoudis, J. Photochem. Photobiol. A 93 (1996) 179.
[10] N. Nahajima, N. Hirota, M. Terazima, J. Photochem. Photobiol. A 120 (1999) 1.
[11] K.O. Ganguin, J. Photo. Sci. 9 (1961) 172.
[12] R.S. Becker, W.F. Richey, J. Chem. Phys. 49 (1968) 2092.
[13] F. Sparatore, G. Pirisino, M.C. Alamanni, P. Manaca-Dimich, M. Satta, Bull. Chim. Farm. 117 (1978) 638.
[14] M. El-Kemary, S. Azim, M. El-Khouly, E. Ebeid, J. Chem. Soc., Faraday Trans. 93 (1997) 63.
[15] M. El-Kemary, M. Fujitsuka, O. Ito, J. Phys. Chem. A 103 (1999) 1329.
[16] M. EI-Kemary, M. El-Khouly, M. Fujitsuka, O. Ito, J. Phys. Chem. A 104 (2000) 1196.
[17] A. Sakrai, H. Midorikawa, Bull. Chem. Soc. Jpn. 41 (1968) 430.
[18] D.F. Eaton, in: J.C. Scaiano, Handbook of Organic Photochemistry, CRC Press, Boca Raton, FL, 1989, Vol. 1, p. 231.
[19] M. Sirish, B.G. Maiya, J. Photochem. Photobiol. A: Chem. 85 (1995) 127.
[20] E.Z. Lippret, Naturforsch. 10a (1955) 541.
[21] E.Z. Lippret, Elektrochemistry 29 (1957) 962.
[22] N. Mataga, Y. Koizumi, Bull. Chem. Soc. Jpn. 29 (1956) 465.
[23] J.A. Dean (Ed.), Lange's Handbook of Chemistry, 13th Edition, McGraw-Hill, New York, 1987.
[24] K. Dimroth, C. Reichardt, T. Siepmann, F. Bohlmann, Liebigs Ann. Chem. 661 (1963) 1.
[25] K.A. Zachariasse, M. Grobys, Th. Von de Haar, A. Hebecker, Yu.V. Il'ichev, O. Morawski, I. Rückert, W. Kühnle, J. Photochem. Photobiol. A: Chem. 105 (1997) 373.
[26] J. Dobkowski, Z. Grabowski, B. Paeplow, W. Rettig, K. Koch, K. Müllen, R. Lapouyade, New J. Chem. 18 (1994) 524.
[27] Z. Grabowski, K. Rotkiewicz, A. Siemiarczuk, D.J. Cowley, W. Baumann, Nouv. J. Chim. 3 (1979) 443.
[28] W. Rettig, J. Mattay (Eds.), Electron transfer I, in: Topics in Current Chemistry, Vol. 169, Springer, Berlin, 1994, p. 253.